Journal of The Electrochemical Society, **164** (6) A961-A967 (2017)
0013-4651/2017/164(6)/A961/7/$37.00 © The Electrochemical Society

Improved Thermal Performance of a Li-Ion Cell through Heat Pipe Insertion

Dean Anthony,[a] Derek Wong,[b] David Wetz,[b,*] and Ankur Jain[a,z]

[a]*Mechanical and Aerospace Engineering Department, University of Texas at Arlington, Arlington, Texas 76019, USA*
[b]*Electrical Engineering Department, University of Texas at Arlington, Arlington, Texas 76019, USA*

Li-ion cells offer excellent energy storage and conversion characteristics, but also suffer from performance and safety problems related to overheating due to insufficient heat removal during operation. Traditional thermal management approaches cool the cell at its outer surface, whereas it is more critical to cool the core of the cell where heat accumulation occurs. This paper investigates thermal performance of a 26650 Li-ion cell with a heat pipe inserted into the core. Heat pipe integrated cells are assembled starting from unfilled, unsealed cells. Thermal benefit of heat pipe insertion is characterized at a number of discharge rates. Advantages of heat pipe cooling compared to traditional surface-based cooling approach are quantified. It is shown that active cooling of the protruding tip of the heat pipe results in maximum thermal benefit, which is shown to reduce the core temperature to as low as, or even lower than the surface temperature. The heat pipe is shown to reduce temperature rise in case of anomalous increase in heat generation. While heat pipe insertion involves significant manufacturing challenges to ensure long-term reliability, the thermal benefits in doing so may potentially outweigh these challenges, and offer an effective thermal management approach for future Li-ion cell designs.

Manuscript submitted November 23, 2016; revised manuscript received February 1, 2017. Published March 9, 2017.

Heat removal from a Li-ion cell is an important technological challenge that directly affects performance, reliability and safety of energy conversion and storage systems, including batteries for consumer electronics, electric vehicles, stationary power systems, etc.[1,2] Heat generated during the operation of a Li-ion cell due to Ohmic losses, electrochemical reactions, etc.[3–5] causes temperature rise. High temperature in a Li-ion cell results in reduced performance and lifetime due to capacity/power fade,[6,7] self-discharge[8,9] and other reasons. Safety of Li-ion cells at high temperatures is also a critical concern due to the well-known phenomenon of thermal runaway,[10,11] in which accelerated heat generation rate at higher temperatures due to a variety of physical and chemical processes may result in an ever-increasing cell temperature,[12] eventually leading to catastrophic failure.[10–13] As a result, it is important to maximize heat removal from a Li-ion cell during operation.

Heat is generated inside a Li-ion cell due to a variety of electrochemical processes occurring within.[3–5,14] Heat generation is usually assumed to be spatially uniform, although there may be somewhat larger heat generation at the metal tabs due to Joule heating. Li-ion cells are traditionally cooled on the outside surface through flow of a cooling fluid such as water or air[1,2] or using a cold plate.[15] In these approaches, heat generated throughout the volume of the cell must be conducted through the cell materials to the surface. The thermal conduction process within the cell is known to be severely impeded by large thermal contact resistances between cell materials inside,[16] resulting in very poor radial thermal conductivity[17,18] and as a result, a large temperature difference between the core of the cell and the outside surface.[19,20] Temperature difference of up to 15°C has been reported for a 26650 cylindrical Li-ion cell discharging at 10C.[21,22] This large temperature difference highlights the challenge in cooling the entire cell volume by surface-based cooling mechanisms. The influence of surface cooling is restricted only to a region close to the surface, whereas cooling is most needed at the core of the cell, which is difficult to thermally access. Some work exists on removing heat internally through current collector tabs,[23] or by pumping electrolyte through the cell to remove heat, effectively using the electrolyte as the cooling fluid.[24] Some work also exists on fabricating microchannels within the volume of the cell and using a cooling fluid for heat removal, although these experiments were not carried out in an actual Li-ion cell.[25] These approaches work better than external cooling in reducing the peak temperature of the cell. However, these approaches are complicated, intrusive and require significant amount of energy, for example, to pump coolant through microchannels in the cell. It is clearly desirable to develop thermal management techniques that directly access the core of the cell, while requiring minimum possible energy for operation.

Insertion of a heat pipe into a Li-ion cell may be an effective strategy for cooling the cell core. A heat pipe is a passive heat transfer device that provides highly directional heat transfer between two bodies.[26–28] A typical heat pipe is a hollow and slender cylinder with the working fluid sealed within. The operation of a heat pipe involves the evaporation of a liquid contained inside due to heat absorption at one end, which then travels along the heat pipe due to buoyancy and capillary action to the condenser end. Heat removal results in condensation back to liquid, which travels back to the evaporator end due to gravity, thereby completing the loop.[26] Fluid flow inside the heat pipe is driven primarily by capillary action in a porous wick structure, making the heat pipe effect possible in any configuration. While the modeling of processes that occur inside a heat pipe is quite involved,[26] the operation of a heat pipe is relatively simple, and does not require active energy input such as pumping. Other advantages include the highly directed nature of cooling, ability to work in constrained space and other challenging environments, and the lack of moving parts. As a result, heat pipes have been used for a variety of thermal management requirements such as cooling of computer microprocessors,[29] photovoltaic cell cooling,[30] high power LEDs[31] and thermal management of electronics in space[32] where convective cooling is not possible.

Recent advances in heat pipe technology, such as oscillating heat pipes[33] and size miniaturization[34] make heat pipes appropriate for thermal management of Li-ion cells. It is still critical, however, to address manufacturing challenges related to the insertion of the heat pipe in an electrochemically active environment inside the cell. The cell needs to remain hermetically sealed despite the presence of the heat pipe, which should not deteriorate the electrochemical performance of the cell. Nevertheless, because the heat pipe directly accesses the core of the cell where cooling is most needed, there may be significant thermal benefits in the use of heat pipes that may justify these additional challenges. A trade-off between thermal benefits and manufacturing challenges may help determine the extent to which heat pipe technology can be integrated with Li-ion cells to prevent thermal runaway and enhance performance.

A limited amount of past research has investigated the use of heat pipes for the cooling of Li-ion battery packs. However, most of this research has focused on inserting heat pipes between cells in a pack, rather than into a cell itself. Thermal benefit of heat pipes placed between cells is somewhat limited. Thermal management of a Li-ion battery pack with heat pipes touching the outside surfaces of cells has been reported.[35] Thermal performance of a flat heat pipe in a battery

*Electrochemical Society Member.
[z]E-mail: jaina@uta.edu

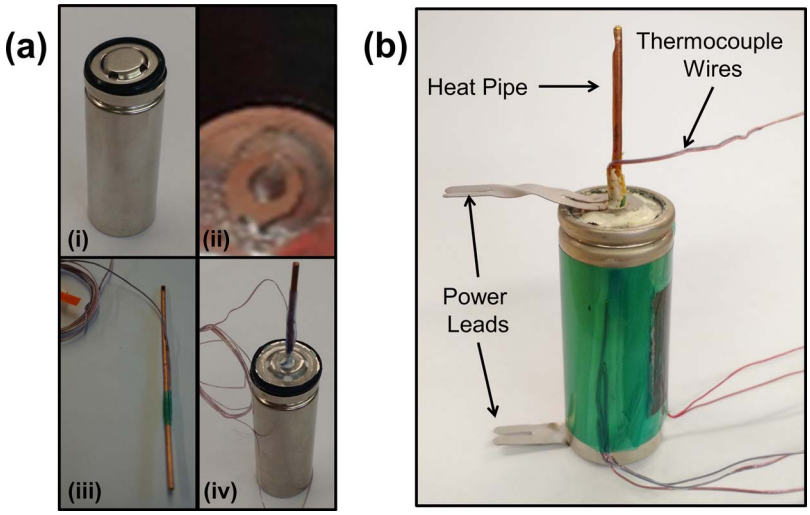

Figure 1. (a) Pictures of various steps in the assembly of a 26650 Li-ion cell with integrated heat pipe; (b) Picture of the final assembled Li-ion cell with heat pipe.

pack has been experimentally and numerically characterized.[36] L-shaped heat pipes have been inserted in battery packs for enhanced cooling.[37] The use of flat heat pipes for cooling of a battery-like heating element on its outside surface has been reported.[38] Numerical optimization of a heat pipe based pack-level thermal management system has been reported.[39] In each of these papers, the heat pipe is located outside the Li-ion cell, and thermal performance is reported in terms of the outside surface temperature. This does not provide much information on the extent of temperature reduction at the core of the cell, where it is most needed. A recent paper reported significant reduction in core temperature upon insertion of a heat pipe into a surrogate thermal test cell similar to a Li-ion cell.[40] However, the insertion of a heat pipe into an actual Li-ion cell has not been reported so far.

This paper carries out experimental investigation into thermal performance enhancement due to a heat pipe inserted in a cylindrical 26650 Li-ion cell. Reduction in core temperature of the Li-ion cell due to the presence of the heat pipe in a variety of operating conditions is reported. Experimental data show that by directing the heat pipe at the core of the cell where temperature is usually the highest and where cooling is most needed, the core temperature can be brought down to as low as the surface temperature, resulting in excellent cooling and thermal uniformity within the cell. The efficacy of heat pipe cooling during discharge at several C-rates is demonstrated. It is also shown that the presence of the heat pipe results in significantly lower core temperature rise in the event of a sudden increase in heat generation rate, such as in a thermal runaway situation. These experimental insights provide a fundamental characterization of thermal performance of heat pipes inserted into Li-ion cells, based on which heat pipe cooling could be evaluated for enhanced safety and performance in future Li-ion cell designs.

Experimental

Assembly of Li-ion cell with integrated heat pipe.—The various steps involved in the assembly of a 26650 Li-ion cell with integrated heat pipe are summarized in Figure 1a. Non-filled, non-sealed, 26650-sized, 2.8 Ah lithium iron phosphate (LFP) cells received from the manufacturer (Figure 1ai) are used to assemble working 26650 cells with integrated heat pipe. 1:1:1 of EC:DEC:DMC with 1 M of $LiPF_6$ salt is used as electrolyte, which is the same formulation used for production cells. The cell has a rated nominal capacity of 2.85 Ah at a charge at half the nominal rate (C/2). The maximum voltage range in which the cell can be cycled is 2.0 V–4.1 V. The maximum continuous charge rate for the cell is 5.7 A while the maximum discharge rate is 50 A. The maximum thermal operating range of these cells is between −40°C and 85°C. In order to accommodate a protruding heat pipe, a hole is drilled from the underside of the top cap through the pressure plate and the top nip (Figure 1aii). The cell is leaned on its side during drilling to avoid metal shavings falling into the jelly roll. A T-type thermocouple is attached at mid-cell height on the outside surface of a 100 mm long, 2 mm diameter heat pipe from Novark Technologies that utilizes deionized water as the working fluid. Note that deionized water does not present the risk of shorting in case of leakage. The heat pipe is then insulated with polyimide tape (Figure 1aiii). The drilled cell and heat pipe are transferred into an Argon glove box. The heat pipe is carefully inserted in the core of the jelly roll (Figure 1aiv). The cell is then mounted upside down and cavities in the top cap are sealed with marine epoxy. The wet epoxy is pushed down in order to fill the cavity between the top nip and the base of the cap. This ensures a proper seal to prevent electrolyte leakage. The cell is left for two hours to allow time for the epoxy to dry completely.

The cell is then filled with 10 mL of electrolyte solution using a 3 mL long needle syringe. The filling is carried out in stages to allow sufficient time for electrolyte to absorb into the films. Once fully filled, the cells are sealed using a set of custom dies fabricated specifically for this cell. Three stages of dies are used to gradually compress the metallic lip around the rubber seal of the top cap. The dies have a through hole in the center to allow the protruding heat pipe to be unharmed during the sealing process. A shunt is inserted between the die and the hydraulic cylinder to protect the protruding heat pipe from bending during this process. The cells are allowed to sit in the glove box for 24 hours to observe for any leaks in the top cap, following which the initial charging of the cells is carried out.

A picture of the final, assembled Li-ion cell with integrated heat pipe is shown in Figure 1b. This picture shows a heat pipe that protrudes about 35 mm out of the top of the cell, as well as thermocouple and power leads.

Electrochemical characterization.—A cell startup procedure is carried out by charging the cell at 0.56 A to 4.1 V using a constant current-constant voltage (CCCV) profile, and a current cutoff of 0.30 A using a Maccor Series 4000 Test System. While the recommended voltage cutoff for this chemistry is normally 3.65 V, the range is extended in order to promote the formation of the solid electrolyte interphase layer on the anode, which is critical to the cycle life of the cell.[41–43] The cell is then cycled five times using the same charging profile, and a constant current discharge at 0.56 A while monitoring cell capacity and checking for signs of electrolyte leakage.

The cell is recharged to 100% state of charge (SOC) and an initial galvanic EIS spectrum is collected from 1 kHz to 5 mHz with a 1.00 A amplitude using a Princeton Applied Research PARSTAT 4000 series potentiostat. A similar characterization is also carried out for a control cell, which is filled and sealed without a heat pipe inserted into

the core. The two EIS spectra shown in the Nyquist plot in Figure 2a indicate very similar electrochemical behavior of the heat pipe cell and a control cell. Figure 2a shows that the heat pipe cell and control cell are similar to each other in the capacitive response across the entire range of scanned frequencies. This indicates that the heat pipe does not adversely affect the capability of the cell to store charge. Further, Figure 2b shows minimal difference between the heat pipe and control cells in terms of the initial charge characteristics. Note that the low frequency Warburg tail of the heat pipe cell in Figure 2a has roughly the same slope as the control cell, indicating that diffusional impedance in the cell is unaffected by the insertion of the heat pipe. The waviness in the tail of the control cell may be explained by the reduction of distance between electrode and separator foils due to insertion of the heat pipe. It should be noted that both cells are cycled initially using a 1C (2.6 A) cycle using a CC-CV charge and a CC discharge profile to grow the initial SEI layers. The growth promotes stability in diffusional transfer. However, with the addition of the heat pipe, there is an uneven gap between the separator foil and the electrodes which may promote the precipitation of SEI products in the heat pipe cell. Thus the control cell has an initial wavy Warburg tail since the SEI has not completely passivated the graphite yet. This is consistently seen in other studies done with these cells. Note that the 1.0 kHz equivalent series resistance (ESR) of the cell with heat pipe is greater than that of the control cell by 21.5 milliohms. Because of this real resistance shift, data in the heat pipe spectrum are normalized along the real impedance axis. This results in the expansion of the mid-frequency semi-circle in the heat pipe cell. This may be explained by slow diffusion of oxygen into the battery through the epoxy resin, causing the breakdown of solvents and conducting salts, thereby increasing the electrolyte resistance. In short, while the procedure to insert the heat pipe does reduce the shelf life of the cell, it is likely to be only due to the imperfect epoxy seal. The heat pipe itself does not appear to interfere with battery charging and discharging processes. However, large-scale implementation of heat pipes in Li-ion cells will require addressing the manufacturing challenge of integrating heat pipe without affecting long-term reliability.

Experimental setup for thermal performance measurements.— The heat pipe-integrated 26650 Li-ion cell is mounted vertically, as shown in Figure 1b, on a thin polystyrene riser to minimize conduction heat loss during experiments. Thermocouples are placed on the outer surface of the cell, at locations L/4, L/2, and 3L/4. The length of the heat pipe protruding out of the top of the cell is 35 mm. An additional large block of polystyrene, with a 2 mm diameter channel capable of completely accommodating the protruding portion of the heat pipe is used as a thermal insulation barrier for insulated heat pipe experiments. Lead wires from a Maccor Series 4000 Automated Test System are attached to the power leads of the cell, shown in Figure 1b. The cell is subjected to a variety of programmable charging and discharging profiles. A Fugetek HT-07530D12 computer fan is used in forced convection experiments to provide active convective cooling. The fan is placed at the same height as the tip of the heat pipe for heat pipe cooling experiments, and at cell mid-height for the cell body cooling experiments. This ensures direct and symmetrical impingement of air from the fan on the surface to be cooled. A variable resistor controller is used for fan speed control. Air speed from the fan is measured using an Extech mini thermo-anemometer. Data acquisition from thermocouples embedded in the core and on the outside of the cell, is carried out using a NI-9213 DAQ thermocouple module, controlled by LabView software. Thermocouple measurements are taken once every second. The measurement rate is appropriate since this system has a much larger time constant than the data acquisition interval.

Thermal performance measurements.— A number of experiments are carried out in a variety of heating and cooling conditions in order to measure the core and outer surface temperatures of the Li-ion cell with embedded heat pipe as functions of time during discharge at various currents. In each case, the Li-ion cell starts fully charged at ambient temperature, and a constant or time-varying discharge load is applied via the Maccor Test System program.

The core and surface temperatures of the cell are measured as functions of time during discharge at a number of discharge currents. In each case, the cell is discharged until the potential difference reaches 2.0 V. In one set of experiments, the protruding tip of the heat pipe is thermally insulated using a polystyrene block. In another set of experiments, the heat pipe tip is cooled through natural convection, without any forced air flow. Finally, these experiments are repeated in the presence of air flow from a fan impinging upon the tip of the heat pipe at various flowrates. In order to compare heat pipe cooling with the traditional approach of outer surface cooling, experiments are also carried out where the air flow impinges upon the outer surface of the cell instead of the heat pipe. Finally, in order to investigate the thermal effect of the heat pipe in a situation of anomalous increase in heat generation, experiments are carried out where a 5 A load is applied for a period of 5 minutes, following by a much larger, 20 A load is applied for the remainder period, which is about 3.5 minutes.

A stabilization time of a few minutes is provided in each experiment involving air flow from the fan before the experiment commences. At the conclusion of each experiment, the cell is charged with a 2.6 A current and allowed to cool for a few hours. The cell is run through an EIS test to ensure that the EIS profile and cell

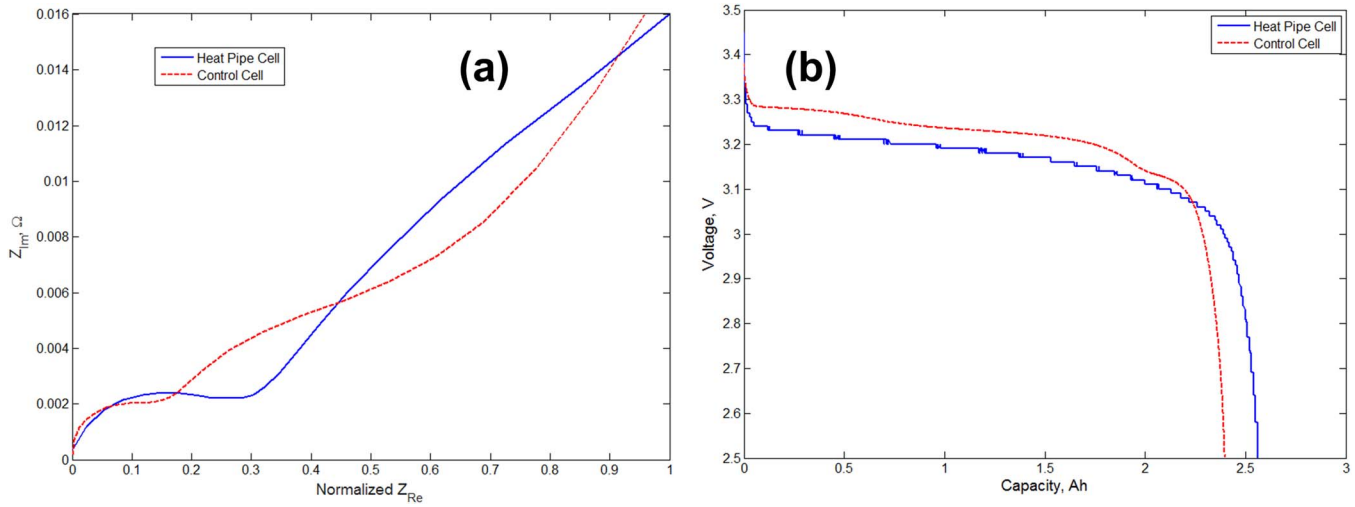

Figure 2. Comparison of (a) Nyquist plot and (b) initial discharge plot for heat pipe integrated Li-ion cell with a control cell that does not contain a heat pipe.

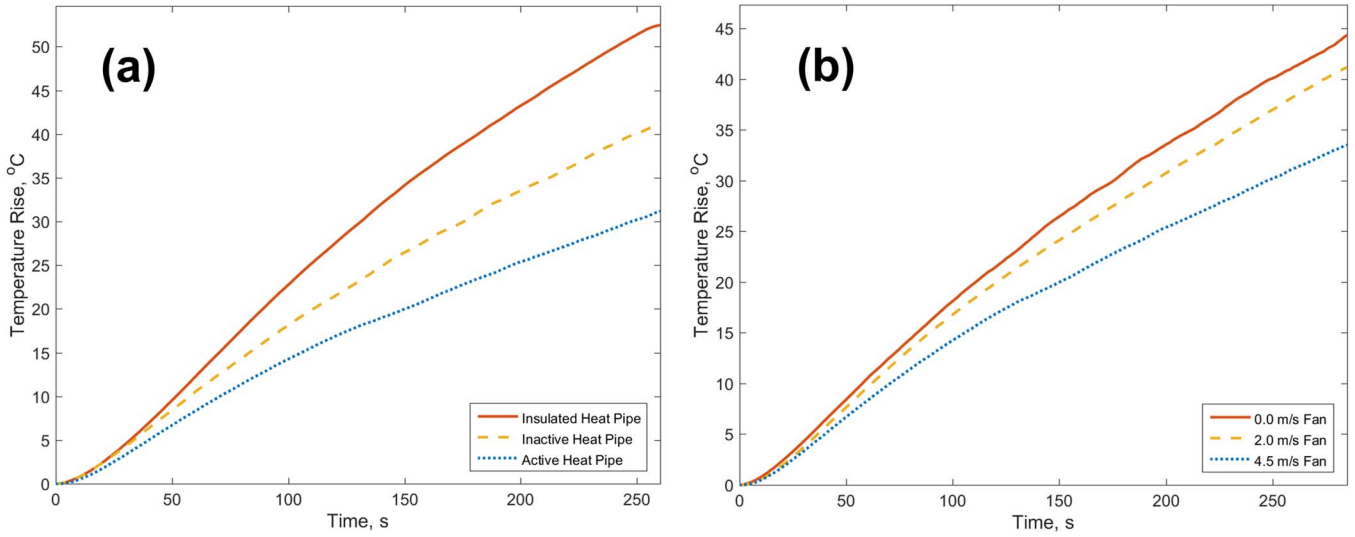

Figure 3. (a) Experimental measurement of core temperature as a function of time during 20 A discharge in three thermal conditions related to tip of the heat pipe – insulated, cooled through natural convection, and actively cooled through forced convection using air flow at 4.5 m/s speed. (b) Experimental measurement of core temperature as a function of time during 20 A discharge during active cooling of the heat pipe tip at three different air flow speeds.

internal resistance have not changed appreciably before proceeding to the next experiment. An extended cool-down period is provided between experiments to ensure that each experiment begins at room temperature.

Results and Discussion

While the embedded heat pipe is capable of transferring heat from the core of the cell to the condenser end located at the tip of the heat pipe, effective use of the heat pipe also requires heat removal from the condenser end. Otherwise, heat accumulation occurs at the condenser end, thereby limiting overall heat pipe effectiveness. To investigate this, thermal performance of the heat pipe is measured in three separate cases. In the first case, the protruding portion of the heat pipe is covered with polystyrene insulation. In the second case, the protruding portion of the heat pipe is exposed to ambient air, so that heat removal occurs through natural convection – this case is referred to as an inactive heat pipe. A fan is used in the third case to provide active convective cooling of the heat pipe tip. Figure 3a plots the measured temperature rise at the core of the cell at mid-height for these cases as functions of time during 20 A discharge, equivalent to about 8C. These data show a significant reduction in temperature rise of up to 20°C between Case 1, where the heat pipe plays no role in cooling due to being insulated, and Case 3, where the heat pipe has the highest thermal effect. Even when the heat pipe is merely inserted without any active cooling of the condenser tip (Case 2), there is substantial improvement in thermal performance compared to the baseline Case 1. Ensuring effective heat removal from the heat pipe tip through forced convection (Case 3) results in the optimal utilization of the heat removal capability of the heat pipe. This is further investigated in experiments where the speed of air flow from the cooling fan is varied. Results plotted in Figure 3b for three different speeds show, as expected, that the temperature of the core reduces as the fan speed increases, due to improved heat removal from the condenser tip of the heat pipe. The reduction in peak temperature shown in Figure 3a due to heat pipe insertion may be approximately represented in terms of an increased effective thermal conductivity of the cell. Based on past analytical heat transfer models for a cylindrical Li-ion cell,[16,20]

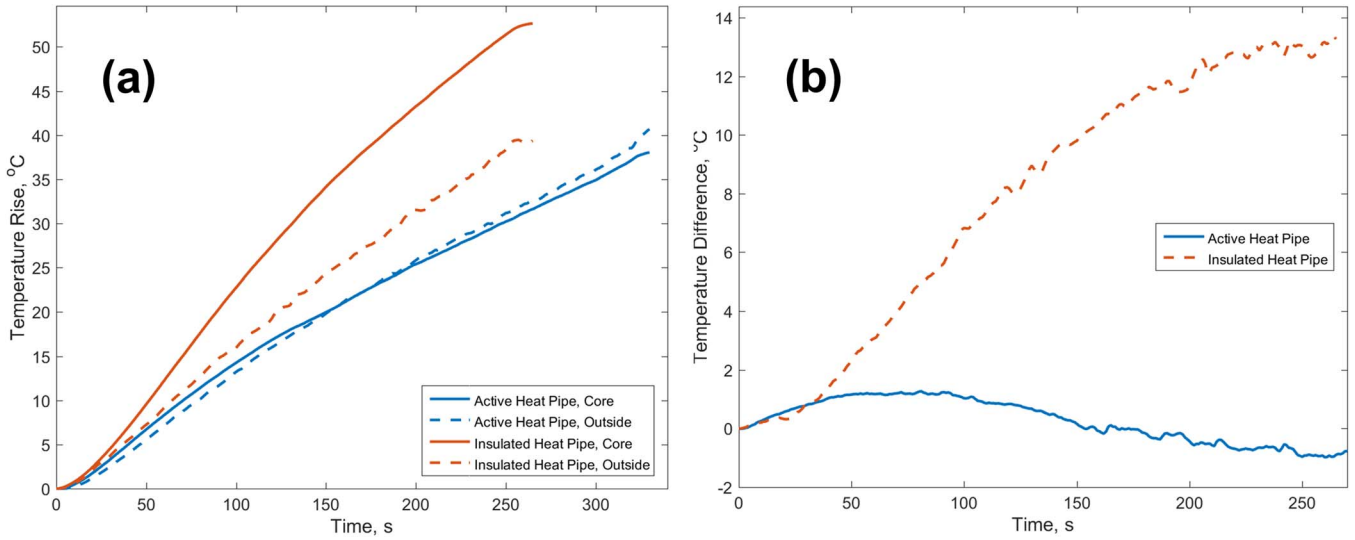

Figure 4. (a) Core and outside surface temperatures as functions of time without and with heat pipe (forced convective cooling) during 20 A discharge, (b) Temperature difference between core and outside surface temperatures.

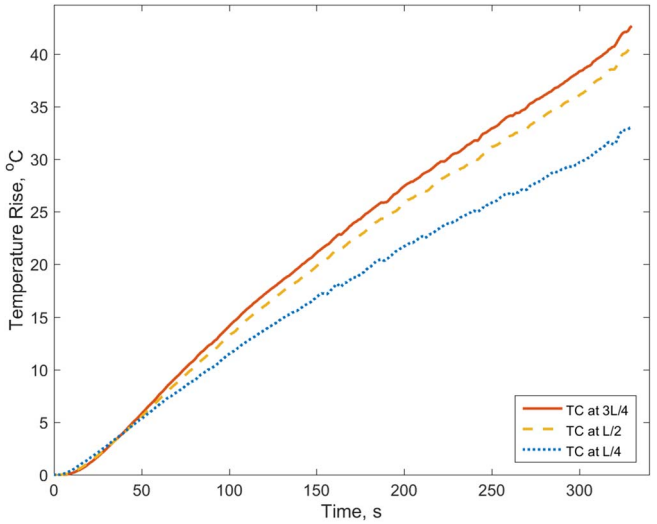

Figure 5. Axial variation in the core temperature during 20 A discharge in the presence of the heat pipe, with forced convective cooling of the heat pipe tip.

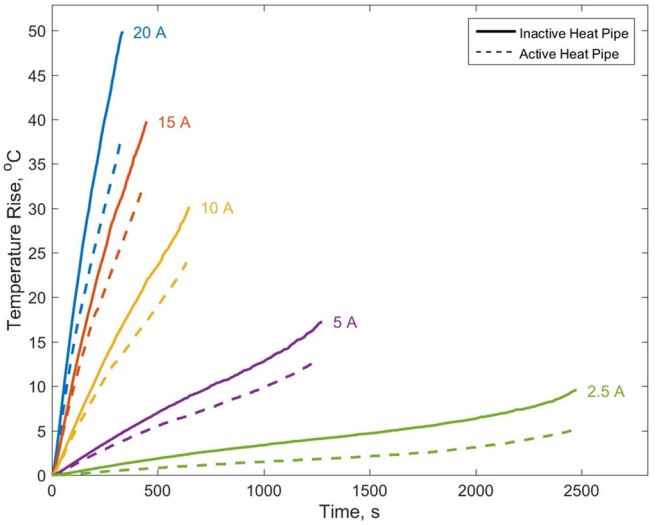

Figure 6. Comparison of core temperatures for multiple discharge rates with inactive and active heat pipe.

it is estimated that heat pipe insertion results in approximately 30% increase in effective thermal conductivity of the cell.

A comparison of the core temperature with the surface temperature of the Li-ion cell is also of interest. It is desirable to bring the two as close to each other as possible in order to minimize spatial temperature gradients within the cell. Figure 4a plots both core and surface temperatures measured as functions of time during 20 A discharge, and compares the temperature response for the cases of insulated and actively cooled heat pipe tip. Compared to the insulated heat pipe tip case, where the heat pipe plays minimal role in heat transfer, the actively cooled heat pipe tip case results in lower values for both core and surface temperatures. Equally importantly, there is a significant temperature difference between the core and surface temperatures in the insulated heat pipe case. This happens because while the outside surface of the cell loses heat to the ambient air, there is no cooling mechanism available at the cell core, which gets much hotter than the surface. On the other hand, when the heat pipe tip is being actively cooled, thereby providing a mechanism for direct heat removal from the core, the core and surface temperatures are very close to each other throughout the discharge period, as shown in Figure 4a. Figure 4b plots the temperature difference between the cell core and surface measured during the discharge process, indicating a gradient of around 13°C by the end of discharge for the insulated heat pipe case, whereas when the heat pipe is actively cooled, the temperature gradient is very small, even negative toward the last half of the discharge process. This interesting result shows that the heat pipe is capable of cooling the core of the cell down to a temperature similar to, or even lower than the surface temperature. This is simply not possible with the current paradigm of cooling cells on the outside surface, which is effective at removing heat close to the cell surface, but not from the core of the cell.

Axial variation in temperature along the core of the cell is also of interest. Figure 5 plots temperature measurement from thermocouples located at three axial locations along the heat pipe inserted in the cell. These data are presented for a 20 A discharge while the tip of the heat pipe is being actively cooled with 4.5 m/s air flow. The thermocouple at three-fourth height – closest to the heat pipe tip – is the hottest, whereas the thermocouple farthest from the heat pipe tip is the coolest. This trend is consistent with the operating principles behind a heat pipe, which indicate that the evaporator section of the heat pipe, farthest away from the condenser tip protruding out from the cell, is expected to have the lowest temperature.[26]

Further experiments are conducted to investigate the importance of effective cooling of the heat pipe tip. In the first set of experiments, the cell is discharged at a number of discharge currents in both inactive and active heat pipe modes. Results summarized in Figure 6 indicate that in each case, the temperature rise in the active heat pipe mode is lower than when the heat pipe is not active. As expected, temperature rise is higher at higher discharge currents due to greater heat generation.

The role of the heat pipe in case of an anomalous increase in heat generation rate from the cell is of interest. Such a scenario may occur, for example, if the cell is thermally or mechanically abused, or if there is a failure of the battery management system. Specifically, an experiment is carried out where the discharge current of the cell suddenly jumps from 5 A to 20 A, representing approximately 16-fold increase in the heat generation rate. Such a large increase in heat generation subjects the cell to a thermal shock, and makes it critical to remove the heat generated in order to prevent large temperature rise leading to thermal runaway. Figure 7 plots the measured core temperature of the cell as a function of time in this scenario for inactive and active heat pipe cases. During the initial phase of the experiment, the two cases are quite similar, with a slightly larger temperature rise in the inactive heat pipe case. However, when the anomalous heat generation occurs, core temperature in the cell with inactive heat pipe rises very rapidly, whereas when the heat pipe is

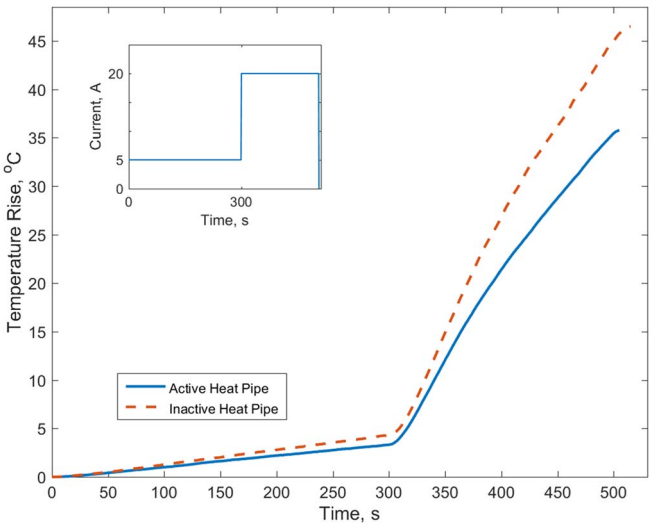

Figure 7. Thermal response of the core temperature to a sudden increase in discharge rate, without and with heat pipe.

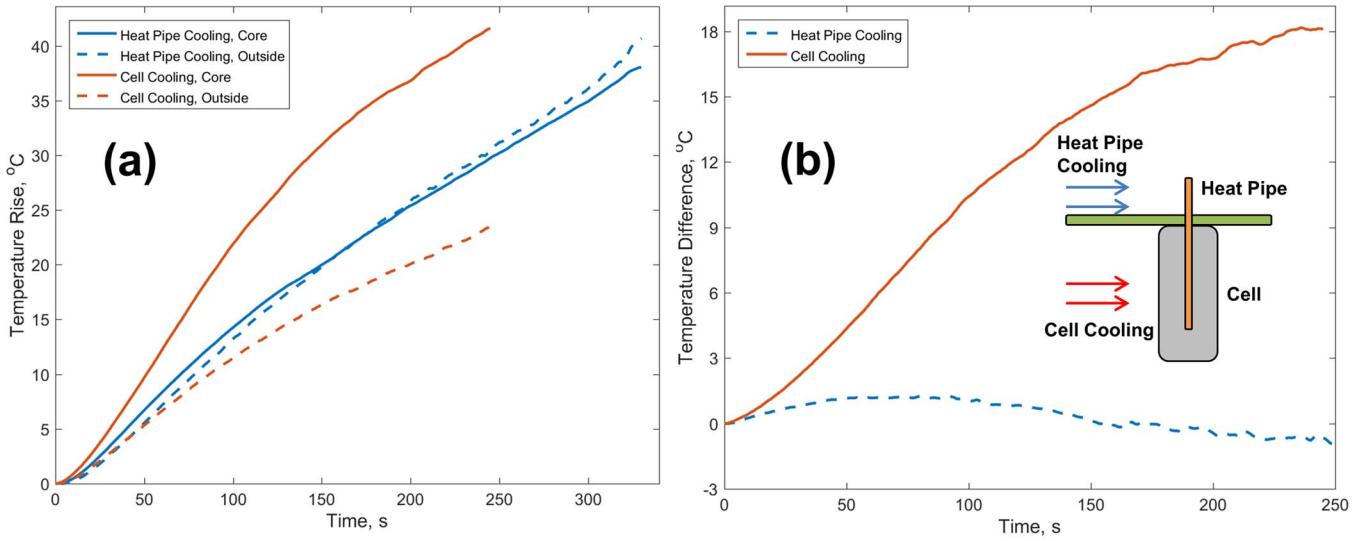

Figure 8. Comparison of (a) core and outside surface temperatures and (b) temperature gradient for heat pipe based cooling with traditional approach of cooling the outer surface.

active, the temperature rise is a lot less steep. Figure 7 shows that within the short period of the anomalous heat generation, temperature rise in the inactive heat pipe case is about 10°C greater than in the active heat pipe case. The temperature difference between the core and surface temperatures of the cell is found to change from 6.7°C (core hotter than surface) without heat pipe to −1.8°C (surface hotter than core) with heat pipe, which also illustrates the beneficial effect of heat pipe insertion.

Finally, heat pipe based cooling is compared with the present paradigm of outer surface-based cooling where coolant flow over the outer surface of the cell results in convective heat transfer. Experiments are carried out where the same air flowrate impinges either over the protruding tip of the heat pipe, or over the cell surface itself, as shown in the inset of Figure 8. Figure 8a plots the measured core and surface temperatures in both cases as functions of time during a 20 A discharge. Direct cell cooling results in a very low cell surface temperature, but fails to similarly reduce the core temperature, primarily due to the large thermal resistance between the core and the surface. On the other hand, when heat pipe cooling is used, the core temperature drops significantly, and, as shown in Figure 8b, the temperature gradient within the cell is much lower throughout the experiment for the heat pipe cooled cell compared to the cell being cooled at the outer surface. This highlights the capability of heat pipe based thermal management to effectively cool the core of the cell, where cooling is most needed, thereby reducing the temperature gradient within the cell.

Conclusions

Heat pipe technology is an attractive approach for reducing operating temperature and improving thermal uniformity in Li-ion cells. This work advances the application of heat pipe in Li-ion cell cooling by inserting a heat pipe into a cell and measuring its thermal benefit during high-rate discharge of the cell. This is a significant improvement over past efforts where the heat pipe was only inserted between cells in a battery pack, because insertion into a cell facilitates heat removal directly from the core of the cell which is in greatest need of cooling. Experiments carried out here show a large temperature reduction due to the presence of the heat pipe, particularly when the protruding tip of the heat pipe is actively cooled in order to promote overall heat transfer. Results indicate that the heat pipe can cause the core temperature to become as low as, or even slightly lower than the outer surface temperature of the cell. Since fluid flow inside a heat pipe does not depend exclusively on gravity, but instead is driven by capillary action in the wick structure, therefore the cooling effects of the heat pipe are expected to be present regardless of whether the cell is vertical, horizontal or in any other configuration.

While the insertion of a heat pipe into a Li-ion cell poses several manufacturing challenges, the experimental data presented in this paper suggests that there may be several thermal benefits in doing so. Further investigation of these manufacturing challenges, particularly to ensure long-term cell reliability in the presence of the heat pipe, is necessary to evaluate this thermal management approach for future Li-ion cell designs. Novel cell designs need to be investigated that accommodate a heat pipe in the cell, for example by providing an axial channel in which to insert the heat pipe. Further, it is also essential to model and optimize the design of the heat pipe itself. This may further improve the thermal performance obtained from the use of heat pipes.

Acknowledgments

This material is based upon work supported by CAREER Award No. CBET-1554183 from the National Science Foundation. Support from Office of Naval Research through grant N00014-16-1-2223 is also gratefully acknowledged. Heat pipe assistance from Dr. Winston Zhang, Novark Technology Inc. is gratefully acknowledged.

References

1. K. Shah, V. Vishwakarma, and A. Jain, *ASME J. Electrochem. Energy Convers. Storage*, **13**, 030801 (2016).
2. T. M. Bandhauer, S. Garimella, and T. Fuller, *J. Electrochem. Soc.*, **158**, R1 (2011).
3. V. Srinivasan and C. Y. Wang, *J. Electrochem. Soc.*, **150**, A98 (2003).
4. K. E. Thomas and J. Newman, *J. Power Sources*, **119**, 844 (2003).
5. D. Bernardi, E. Pawlikowski, and J. Newman, *J. Electrochem. Soc.*, **132**, 5 (1985).
6. M. Broussely, in *Advances in Lithium-Ion Batteries*, W. A. V. Schalkwijk and B. Scrosati, Editors, P. 393, Kluwer Academic/Plenum Publishers, New York (2002). ISBN 978-0-306-47508-5.
7. P. Arora, R. E. White, and M. Doyle, *J. Electrochem. Soc.*, **145**, 3647 (1998).
8. D. Aurbach, *J. Power Sources*, **146**, 71 (2005).
9. B. A. Johnson and R. E. White, *J. Power Sources*, **70**, 48 (1998).
10. Q. Wang, P. Ping, X. Zhao, G. Chu, J. Sun, and C. Chen, *J. Power Sources*, **208**, 210 (2012).
11. R. Spotnitz and J. Franklin, *J. Power Sources*, **113**, 81 (2003).
12. K. Shah, D. Chalise, and A. Jain, *J. Power Sources*, **330**, 167 (2016).
13. H. Maleki, G. Deng, A. Anani, and J. Howard, *J. Electrochem. Soc.*, **146**, 3224 (1999).
14. Y. Ye, Y. Shi, N. Cai, J. Lee, and X. He, *J. Power Sources*, **199**, 227 (2012).
15. N. Nieto, L. Diaz, J. Gastelurrutia, F. Blanco, J. C. Ramos, and A. Rivas, *J. Power Sources*, **272**, 291 (2014).
16. V. Vishwakarma, C. Waghela, Z. Wei, R. Prasher, S. C. Nagpure, J. Li, F. Liu, C. Daniel, and A. Jain, *J. Power Sources*, **300**, 123 (2015).
17. S. J. Drake, D. A. Wetz, J. K. Ostanek, S. P. Miller, J. M. Heinzel, and A. Jain, *J. Power Sources*, **252**, 298 (2014).

18. J. Zhang, B. Wu, Z. Li, and J. Huang, *J. Power Sources*, **259**, 106 (2014).
19. K. Shah, S. J. Drake, D. A. Wetz, J. K. Ostanek, S. P. Miller, J. M. Heinzel, and A. Jain, *J. Power Sources*, **271**, 262 (2014).
20. K. Shah, S. J. Drake, D. A. Wetz, J. K. Ostanek, S. P. Miller, J. M. Heinzel, and A. Jain, *J. Power Sources*, **258**, 374 (2014).
21. S. Drake, M. Martin, D. A. Wetz, J. K. Ostanek, S. P. Miller, J. M. Heinzel, and A. Jain, *J. Power Sources*, **285**, 266 (2015).
22. C. Forgez, D. V. Do, G. Friedrich, M. Morcrette, and C. Delacourt, *J. Power Sources*, **195**, 2961 (2010).
23. S. J. Bazinski and X. Wang, *J. Electrochem. Soc.*, **161**, A2168 (2014).
24. S. K. Mohammadian, Y. L. He, and Y. Zhang, *J. Power Sources*, **293**, 458 (2015).
25. T. M. Bandhauer and S. Garimella, *Appl. Therm. Eng.*, **61**, 756 (2013).
26. A. Faghri, *J. Heat Transfer*, **134**, 123001 (2012).
27. S. W. Chi, *Heat pipe theory and practice: a sourcebook*, Hemisphere Publishing Corporation, Washington, DC (1976). ISBN: 0070107181.
28. P. D. Dunn and D. A. Reay, *Heat Pipes*, 3rd ed., Pergamon Press Inc., New York (1982). ISBN: 0080293565.
29. R. Mahajan, C. P. Chiu, and G. Chrysler, *Proc. IEEE*, **94**, 1476 (2006).
30. A. Akbarzadeh and T. Wadowski, *Appl. Therm. Eng.*, **16**, 81 (1996).
31. X. Y. Lu, T. C. Hua, M. J. Liu, and Y. X. Cheng, *Thermochim. Acta*, **493**, 25 (2009).
32. R. R. Riehl and T. Dutra, *Appl. Therm. Eng.*, **25**, 101 (2005).
33. H. B. Ma, B. Borgmeyer, P. Cheng, and Y. Zhang, *J. Heat Transf.*, **130**, 081501 (2008).
34. V. Y. Kravets, Y. E. Nikolaenko, and Y. V. Nekrashevich, *Heat Transf. Res.*, **38**, 553 (2007).
35. Z. Rao, S. Wang, M. Wu, Z. Lin, and F. Li, *Energy Convers. Manag.*, **65**, 92 (2013).
36. T. H. Tran, S. Harmand, B. Desmet, and S. Filangi, *Appl. Therm. Eng.*, **63**, 551 (2014).
37. Q. Wang, B. Jiang, Q. F. Xue, H. L. Sun, B. Li, H. M. Zou, and Y. Y. Yan, *Appl. Therm. Eng.*, **88**, 54 (2014).
38. N. Putra, B. Ariantara, and R. A. Pamungkas, *Appl. Therm. Eng.*, **99**, 784 (2016).
39. Y. Ye, L. H. Saw, Y. Shi, and A. A. O. Tay, *Appl. Therm. Eng.*, **86**, 281 (2015).
40. K. Shah, C. McKee, D. Chalise, and A. Jain, *Energy*, **113**, 852 (2016).
41. M. Rashid and A. Gupta, *J. Electrochem. Soc.*, **162**, A3145 (2015).
42. M. Rashid and A. Gupta, *ECS. Electrochem. Lett.*, **3**, A95 (2014).
43. A. Mabuchi, K. Tokumitsu, H. Fujimoto, and T. Kasuh, *J. Electrochem. Soc.*, **142**, 1041 (2000).